THE JOURNAL OF PHYSICAL CHEMISTRY B

Article

pubs.acs.org/JPCB

Transferable Force Field for Equilibrium and Transport Properties in Linear and Branched Monofunctional and Multifunctional Amines. II. Secondary and Tertiary Amines

Gustavo A. Orozco,[†,‡] Carlos Nieto-Draghi,[†] Allan D. Mackie,[‡] and Véronique Lachet*[,†]

[†]IFP Energies nouvelles, 1-4 avenue de Bois-Préau, 92852 Rueil-Malmaison, France

[‡]Departament d'Enginyeria Química, ETSEQ, Universitat Rovira i Virgili, Av. dels Països Catalans 26, 43007 Tarragona, Spain

Supporting Information

ABSTRACT: Following the same philosophy of our previous force field for primary amines (*J. Phys. Chem. B* **2011**, *115*, 14617), we present an extension for secondary and tertiary amines using the anisotropic united atom (AUA4) approach. The force field is developed to predict the phase equilibrium and transport properties of secondary and tertiary amines. The transferability was studied for an important set of molecules including as secondary amines dimethylamine, diethylamine, di-*n*-propylamine, di-iso-propylamine, and di-iso-butylamine. We have also tested diethylenetriamine, a multifunctional molecule which includes two primary and one secondary amino groups. For tertiary amines, we have included simulations for trimethylamine, triethylamine, tri-*n*-propylamine, and methyldiethylamine. Monte Carlo simulations in the Gibbs ensemble were carried out to study thermodynamic properties such as equilibrium densities, vaporization enthalpies, and vapor pressures. Critical coordinates (critical density and critical temperature) and normal boiling points were also calculated. The shear viscosity coefficients were studied for dimethyl, diethyl, di-*n*-propyl, trimethyl, triethyl, and tri-*n*-propylamine at different temperatures using molecular dynamics in the isothermal isobaric ensemble. Our results show a very good agreement with experimental values for all the studied molecules for both thermodynamic and transport properties, demonstrating the transferability of our force field.

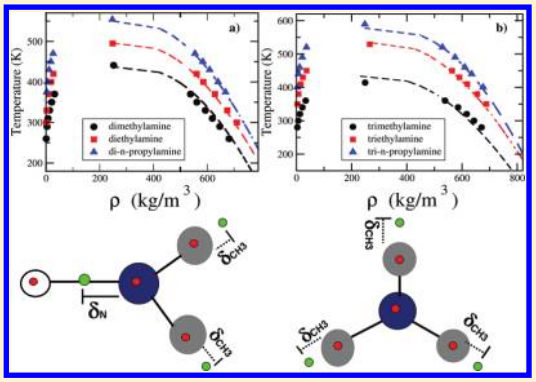

1. INTRODUCTION

Amines play an essential role in the development of CO_2 capture and sweetening gas technologies. Given that these technologies are based on separation operations, knowledge of the relevant transport and the thermodynamic parameters is of vital importance to model and optimize the corresponding processes. Besides classical equations of state, molecular simulation is nowadays a real alternative to estimate thermodynamic properties. Molecular simulation has many advantages for properties estimation, particularly where the experimental conditions are difficult to carry out because of factors such as extreme operating conditions of pressure and temperature, risk of toxicity, presence of hazardous chemical components, or when the experimental setups are prohibitively expensive. In addition, molecular simulation also allows transport properties to be predicted, or to explore the molecular structure of the system. Nevertheless, in order to be able to estimate thermodynamic or transport properties by means of molecular simulation, force fields are necessary. These force fields provide both the intra- and intermolecular energies, i.e., the interactions between the atoms of the same molecules and between the different molecules in a specific phase, respectively.

Several molecular simulation studies have already been published for amines, where primary amines have been studied the most. However, in the case of secondary and tertiary amines, transferable force fields are scarce. Indeed, only two transferable potentials are currently available, both of which are all atom approaches, which implies that all the atoms are explicitly included. It is also worth pointing out that, compared with primary amines, there is much less experimental information available for phase equilibrium properties.

The first transferable force field proposed for amines, which includes primary, secondary, and tertiary amines, was proposed by Rizzo et al.[1] In this work, a set of Lennard-Jones (L-J) parameters and partial charges are calculated by fitting to experimental data for pure liquids and to the hydrogen bond strength from gas-phase ab initio calculations. This is an all atom potential (AA) known as OPLS-AA (optimized potential for liquid simulations-all atom), which includes 8 and 10 partial charges located on the corresponding amino group for secondary and tertiary amines, respectively. Their study includes four linear amines, namely, dimethylamine, diethyl-

Received: March 28, 2012
Revised: April 17, 2012
Published: May 2, 2012

ACS Publications © 2012 American Chemical Society

amine, trimethylamine, and triethylamine. The second force field follows the TraPPE-EH approach (transferable potential for phase equilibria-explicit hydrogens).[3] Wick et al. carried out simulations in the Gibbs ensemble at different temperatures and studied the same molecules as in the OPLS-AA force field. Nonbonded interaction parameters were fitted in order to reproduce the experimental vapor−liquid curves. No average deviations are presented in this work; however, based on the simulation values that can be found in their Supporting Information, we have calculated global average deviations with respect to experimental information. We find for their four studied molecules average deviations of 1% for liquid densities and 21% for vapor pressures. In the case of vaporization enthalpies, it was not possible to make the same comparison because only one value is reported for each molecule. For the normal boiling point, deviations of 1.3% were found for the four studied molecules. Wick and co-workers have also presented a comparison between their results and the ones belonging to the OPLS-AA force field. They conclude for the studied molecules that the OPLS-AA liquid densities agree well with the experimental values but only close to the boiling point, showing important deviations as the temperature is increased. In addition, Wick has reported deviations larger than 10% for the critical point estimation using the OPLS-AA force field for amines.

Additional works have been presented for secondary amines. For example, Schnabel et al.[4] proposed a rigid model for both dimethylamine and diethylamine, using a different geometry for the amino group of the two studied molecules. They transferred the AUA4 potential for hydrocarbons[5] to model the carbons present in the chain and reoptimized a set of charges and Lennard-Jones parameters for the amino group. As a result, they reported a good agreement for the studied properties. Unfortunately, they did not extend their study to tertiary amines and no further amine molecules were studied. Furthermore, their model cannot be straightforwardly applied to long chain and bifunctional molecules due to the fact that they consider rigid molecules. Since different bond lengths and angles are used for each molecule, the model cannot be considered as being transferable for other amines. Finally, Baskaya et al.[6] presented a model for secondary amines and studied three amine molecules—dimethyl, diethyl, and di-*n*-propylamine—using discontinuous step potentials with molecular dynamics obtaining deviations of 4% in the density estimations.

Sumarizing, only a few short molecules have been studied in the previous works, and the transferability of these models to longer, branched or multifunctional amines has not been checked. This point is exacerbated due to the lack of torsional potentials for nonlinear and short multifunctional amines, making it difficult to study such molecules. Finally, to our knowledge, none of the available transferable force fields have checked the corresponding transport properties.

A force field can be classified according to the number of force centers used: (i) all atom (AA), where all the atoms present in a molecule are taken into account, (ii) united atom (UA), where only one force center per functional group is considered, located at the center of the main atom of the functional group, and, finally, (iii) anisotropic united atom (AUA), first proposed by Toxvaerd[7] and reparametrized by Ungerer,[8] which differs with UA in the location of the force center. Here, the force center is displaced from the central atom toward the hydrogens of the group. Different AUA force fields have been presented, initially for hydrocarbons (AUA4)[9−16] and later on for different functional groups[17−23] including a recently proposed force field for primary amines.[24] In the case of the AUA4 approach, we can mention the following advantages: the number of force centers is significantly reduced compared with AA models, vapor pressures and vaporization enthalpies have been found to give better results than other available models, and finally, in the case of primary amines,[24] a substantial number of torsions have been included in order to allow the force field to be transferable to a large set of molecules.

The aim of this work is to present a transferable force field for secondary and tertiary amines, applicable to a large variety of molecules, and able to reproduce both thermodynamic equilibrium properties and transport coefficients such as viscosity. In addition, the transferability of the force field for different types of molecules is shown, including not only short or linear molecules but also more complex branched and multifunctional molecules. This article is divided up as follows: first, we present the details relating to the force field development, i.e., electrostatic and L-J interactions, torsional potentials, etc., together with the simulation details. Afterward, in the Results section, we present the transferability of the force field in estimating properties for several molecules including both thermodynamic and viscosity coefficients. Finally, the conclusions are presented in the fourth section.

2. FORCE FIELD DEVELOPMENT

2.1. Proposed Model and Nonbonded Interactions.

Figure 1 gives a schematic representation of our proposed AUA4 model for secondary and tertiary amines, using dimethyl and trimethylamine as examples. As shown, for secondary amines and in particular dimethylamine (top), four charges (red filled circles) are chosen, located on atoms. In addition, three force centers (green filled circles) are used. Two of these force centers correspond to the methyl groups, and are located according to the AUA4 force field rules for hydrocarbons.[5] The third and last force center is located on the amino group along the N−H bond at a δ displacement from the nitrogen atom.

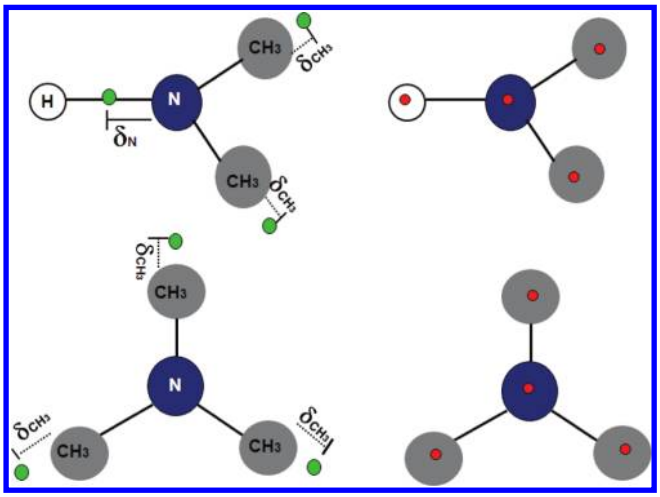

Figure 1. Schematic representation of the AUA4 force field for secondary (top) and tertiary (bottom) amines. Green filled circles represent Lennard-Jones force centers (first column), while red filled circles represent the partial charges (second column).

dx.doi.org/10.1021/jp302972p | J. Phys. Chem. B 2012, 116, 6193−6202

For tertiary amines and in particular trimethylamine (bottom of Figure 1), four charges and four L-J groups are proposed. Unlike secondary amines, the corresponding force center of the amino group is located on the nitrogen atom, since all the hydrogens are substituted by methyl or methylene groups. For larger molecules, for instance, diethylamine, more methyl or methylene groups have to be added, locating the force centers according to the AUA4 rules (depending on the number of bonded hydrogens in the functional group). The manner in which the force field parameters were obtained, i.e., charges and Lennard-Jones parameters, will be explained later in this section together with their numerical values.

Thus, our proposed model for secondary amines is made up of only three new adjustable parameters (σ, ϵ, and δ) for the dispersion−repulsion of the amino group. For tertiary amines, only two new adjustable parameters are needed corresponding to σ and ϵ of the amino group. Parameters for the hydrocarbons were taken directly from the AUA4 force field for hydrocarbons.[5]

Nonbonded interactions between two force centers are calculated using a 12-6 Lennard-Jones (L-J) potential, eq 1, while electrostatic interactions are calculated using Coulomb's law, eq 2, where q_i and q_j represent the partial charges on the molecule and ϵ_o the vacuum permittivity.

$$U^{\text{L-J}}(r_{ij}) = 4\epsilon\left[\left(\frac{\sigma_{ij}}{r_{ij}}\right)^{12} - \left(\frac{\sigma_{ij}}{r_{ij}}\right)^{6}\right] \quad (1)$$

$$U^{\text{electrostatic}} = \frac{q_i q_j}{4\pi\epsilon_o r_{ij}} \quad (2)$$

Cross interactions were obtained using the Lorentz−Berthelot combining rules:

$$\epsilon_{ij} = \sqrt{\epsilon_{ii}\epsilon_{jj}} \quad (3)$$

$$\sigma_{ij} = \frac{1}{2}(\sigma_{ii} + \sigma_{jj}) \quad (4)$$

The Lennard-Jones parameters for the amino group were obtained through a numerical optimization, while all the L-J parameters for the hydrocarbons were taken from the AUA4 potential.[5] Table 2 summarizes the nonbonded parameters used in our model. As explained by Ungerer et al.,[8] the AUA4 parameters for hydrocarbons follow a physically correct tendency; for instance, there is a regular evolution of both σ and ϵ when the number of hydrogens decreases in the group,

Table 1. Partial Charges

force center	q	ref
CH_x[a]	+0.180 if bonded to 1° amine	24
	+0.176 if bonded to 2° amine	this work
	+0.230 if bonded to 3° amine	this work
	0 elsewhere	
N(1° amine)	−0.892	3
N(2° amine)	−0.730	this work
N(3° amine)	−0.690	this work
H(1° amine)	+0.356	3
H(2° amine)	+0.378	this work

[a]These values correspond to the partial charge located on the α-carbon of the amino group.

Table 2. Nonbonded Lennard-Jones Parameters

force center	ϵ (K)	σ (Å)	δ (Å)	ref
CH_3	120.15	3.607	0.216	5
CH_2	86.29	3.461	0.384	5
CH	50.98	3.363	0.646	5
N(1° amine)	137.46	3.415	0.170	24
N(2° amine)	120.66	3.172	0.497	this work
N(3° amine)	47.00	2.600	0	this work
H(N)	0	0	0	this work

i.e., CH_3, CH_2, and CH. For the studied amines, i.e., primary, secondary, and tertiary, note that the set of parameters presented also follows a correct trend, where the energy as well as the van der Waals radius decreases as the number of hydrogens decreases, i.e., NH_2, NH, and N.

Charges and Electrostatic Intermolecular Energy. In order to choose a consistent set of charges for the involved amino groups, we have performed quantum calculations using the density functional theory (DFT) at the B3LYP level, 6-311** as a basis set and Jaguar[25] as the computational tool. We have studied the magnitude of the dipole moment both in the vapor phase and in the liquid phase. Calculations for the liquid phase were done using Jaguar's solvation model (Poisson−Boltzmann solver, PB) which fits the field produced by the solvent dielectric continuum to a set of point charges. Experimental information was required,[2,26−29] such as dielectric constant, density, and molecular weight.

Figure 2 presents the behavior of the dipole moments in Debye for both secondary and tertiary amines in the gas phase

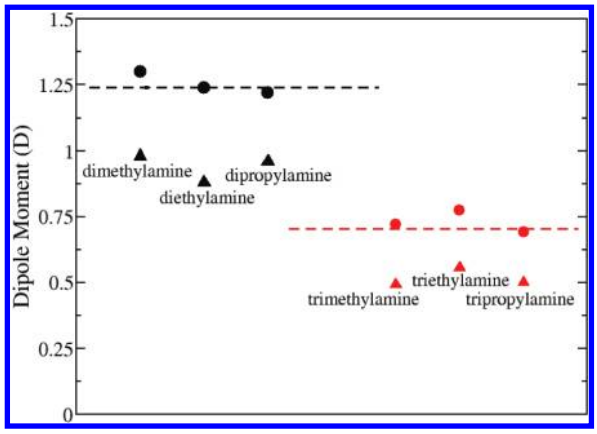

Figure 2. Comparison between gas and liquid dipole moments for secondary (black) and tertiary (red) amines, obtained by DFT calculations. Triangles represent the gas phase, while filled circles, the liquid phase. The dashed lines indicate the calculated dipole moments using the proposed charges from our force field.

(triangles) and in the liquid phase (filled circles). From this figure, it is possible to infer that a different set of charges is needed for secondary and tertiary amines, due to the fact that the difference between the dipole moments in the liquid phases is around 85%. On the other hand, since relatively small variations of the dipole moment are found within the secondary amine series and within the tertiary amine series, we assumed that the dipole moment was constant within a given series. In the case of the primary amine series, the same approximation was also used.[24] For both secondary and tertiary amines, the

dx.doi.org/10.1021/jp302972p | J. Phys. Chem. B 2012, 116, 6193−6202

dashed line represents the dipole moment behavior using the set of charges proposed in this work.

For multifunctional molecules such as diethylenetriamine (DETA), it is necessary to calculate intramolecular electrostatic interactions. Here we have employed the local dipole approach proposed by Ferrando.[20] This approach was also used in our previous work on primary amines where bifunctional amines such as ethylenediamine, among others, were studied. The advantages of using the local dipole calculation are basically that neither additional interaction terms nor scaling factors need to be considered.

2.2. Intramolecular Energy. With regards to the bonded intramolecular interactions, our proposed force field considers that (i) all bonds are rigid, (ii) groups of three connected atoms interact by means of a harmonic bending potential, and, finally, (iii) groups of four connected atoms interact by way of a torsional potential which is a function of the corresponding dihedral angle. Interactions between force centers separated by more than three bonds were considered via the same L-J potential as for intermolecular interactions, eq 1. For multifunctional amines, 1-4 intramolecular L-J interactions were also considered.

For the hydrocarbon groups, bond lengths were taken from the AUA4 force field for alkanes,[8] while, for the amino group, the N−H bond was taken from ref 1 and the C−N from ref 30. A bending potential given by eq 5 was used, where k_{bend} is the bending constant and θ and θ_0 are the bending and equilibrium bending angles, respectively. The primary amine HNH, CNH, and CCN bending parameters were taken from our previous work.[24] For secondary and tertiary amines, the equilibrium angles were chosen from the experimental information related to the molecular structure.[30−34] Tables 3 and 4 summarize all the information with regard to bond lengths and bending parameters.

$$U_{bending} = \frac{1}{2}k_{bend}(\cos\theta - \cos\theta_o)^2 \quad (5)$$

Interactions between four connected atoms were calculated as a function of the dihedral angle (ϕ) using the torsional potential given by eq 6, where χ is defined such that $\chi = \phi + 180°$.

$$U_{tor}(\chi) = \sum_{i=0}^{8} a_i[\cos(\chi)]^i \quad (6)$$

Besides the torsional potentials already developed for primary amines, additional torsions for secondary and tertiary amines were also calculated. It is important to mention that the currently available force fields for amines (see the Introduction) use the same torsional potentials for secondary and tertiary amines. In particular, the torsional potential $CH_x-CH_2-NH-CH_x$ for secondary amines is considered equal to the corresponding one for tertiary amines $CH_x-CH_2-N-CH_x$. In this work, we have fitted a different torsional potential for secondary and tertiary amines. Furthermore, for branched amines such as di-iso-propylamine, we have also proposed an additional torsion. In total, three torsions have been proposed, corresponding to $CH_x-CH_2-NH-CH_x$ for secondary amines, $CH_x-CH_2-N-CH_x$ for tertiary amines, and $CH_x-CH-NH-CH_x$ for secondary branched amines. In the following, we will explain the procedure used to calculate the torsions.

In order to calculate the coefficients of the three new torsion potentials given in Table 5, we have used diethylamine, methyldiethylamine, and di-iso-propylamine as reference molecules. A similar procedure to the one proposed for primary amines was used. Briefly, the total energy of the molecule in its ground state was calculated at different conformations of the dihedral angle between 0 and 360° obtained from a quantum calculation. Afterward, and at each conformation, all the other energy contributions such as bending energies, intramolecular L-J, intramolecular electrostatic interactions, and other torsional energies involving other dihedral angles, were subtracted from the total energy. Once the torsional energy is calculated at each conformation, it is possible to obtain the a_i coefficients by a fitting procedure. Table 5 summarizes the coefficients after the fitting procedure. The total energy was computed with both DFT and a second-order Moller−Plesset perturbation theory (MP2), where no significant differences between them were found. Calculations were performed with the Jaguar[25] software.

2.3. Simulation Details. The simulations were performed using the in-house GIBBS Monte Carlo code developed by IFPEN and Orsay University.[5] Gibbs ensemble simulations at constant volume and temperature with periodic boundary

Table 3. Bond Lengths

bond	r_0(Å)	ref
H−N	1.010	1
C−N	1.463	30
C−C	1.535	8

Table 4. Bending Parameters

angle	k_{bend} (K)	θ_0 (deg)	ref
CH_x-N-H	39642	109.50	1
H−N−H	47681	106.40	1
C−C−N	63630	109.47	1
$CH_x-CH_2-CH_x$	74900	114.00	8
$CH_x-CH-CH_x$	72700	112.00	8
$CH_x-NH-CH_x$	57128	112.30	30
CH_x-N-CH_x	57128	111.00	30

Table 5. Calculated Torsions $U_{tor}(\chi) = \sum_i a_i \cos(\chi)^i$

torsion	a_0 (K)	a_1 (K)	a_2 (K)	a_3 (K)	a_4 (K)	a_5 (K)	a_6 (K)	a_7 (K)	a_8 (K)	ref
CH_x-CH_2-N-H	154.98	869.66	902.48	−586.65	−651.38	−607.86	253.22	149.74	102.90	24
$CH_x-CH-N-H$	60.65	238.22	218.52	−114.57	−353.18	−267.63	291.94	99.18	−71.84	24
$CH_x-CH_2-NH-CH_x$	134.01	1028.60	1427.94	−1739.77	−960.76	−106.72	693.93	−177.42	−170.38	this work
$CH_x-CH-NH-CH_x$	282.03	444.56	179.41	−1035.08	560.51	361.84	−1415.75	−330.23	811.53	this work
$CH_x-CH_2-N-CH_x$	189.01	979.05	1482.82	−1436.82	−1465.09	−1219.26	913.04	541.13	16.99	this work
$CH_x-CH_2-CH_2-N$	816.65	2509.94	9.01	−3609.00	−54.51	286.01	−104.22	−133.18	279.10	24
$CH_x-CH-CH_2-N$	546.87	1367.99	−26.97	−2344.08	−817.65	987.54	−1163.02	−624.30	−340.10	24
$N-CH_2-CH_2-N$	1438.78	3531.87	−548.67	−3550.53	−1561.15	−1733.35	4323.74	933.26	−1997.11	24

dx.doi.org/10.1021/jp302972p | J. Phys. Chem. B 2012, 116, 6193−6202

conditions and the minimum image convention were used. To calculate the L-J interactions between force centers, a spherical cutoff equal to half of the simulation box was applied, while for long-range electrostatic interactions the Ewald procedure was chosen[35] with a maximum of seven vectors in each direction of reciprocal space and with the scaling parameter $\alpha = 2$ in reduced units. In order to sample the configurational phase space, different MC moves were used, including translations (20%), rigid rotations (20%), configurational bias regrowths (20%), transfers with insertion bias (39.5%), and volume changes (0.5%). In order to improve the sampling for larger secondary amines such as di-iso-butylamine and DETA, we used translations (15%), configurational bias regrowths (15%), internal rotations (15%) (i.e., the rotation of a force center around its nearest neighbors), pivots (15%), transfers with insertion bias (39.5%), and volume changes (0.5%). We used the same moves for tertiary amines as for secondary amines, except for trimethylamine where internal rotations were not included. The amplitudes of translations, rotations, and volume changes were adjusted during the simulation to achieve an acceptance ratio of 40% for these moves.

Most of the simulations were performed using 10 million Monte Carlo steps (MCS) for the equilibration part and 50 million for the production part, where one MCS corresponds to a simple Monte Carlo move. For longer molecules such as di-*n*-propylamine, tri-*n*-propylamine, and DETA, longer simulations ranging between 80 and 120 million MCS were employed. Nearly all the boxes contained a total of 350 molecules, except for temperatures close to the critical point, where the size of the system was increased up to 600 molecules. Normal boiling points (T_b) were estimated by fitting the vapor pressures (P_v) to the Clausius−Clapeyron equation, eq 7, at different temperatures, where C and D are constants.

Critical densities ρ_c and critical temperatures T_c were calculated by means of a scaling law, eq 8, and the law of rectilinear diameters, eq 9:

$$\ln P_v = \frac{C}{RT} + D \tag{7}$$

$$\rho_L - \rho_V = A(T_c - T)^{\beta^*} \tag{8}$$

$$\frac{\rho_L + \rho_V}{2} = \rho_c + B(T_c - T) \tag{9}$$

where ρ_L and ρ_V correspond to the liquid and vapor densities, β^* is a characteristic universal exponent (for this work, $\beta^* = 0.325$[35]), and A and B are adjusted parameters.

Viscosity coefficients were calculated using molecular dynamics. In this case, the equations of motion were integrated by way of the velocity Verlet algorithm with constrained bonds using the Rattle algorithm.[36] The simulations were performed in the NPT ensemble using both the Berendsen barostat and thermostat. Equilibration runs of 1 ns were used, while runs of 5 ns were applied for the production part. In both cases, the integration time step was 2 fs. A Verlet nearest neighbor list was also included in order to improve the performance of the simulations. In all cases, 300 molecules were placed in a cubic box with periodic boundary conditions. To estimate the viscosity coefficients, both the Einstein and Green−Kubo formalisms were applied. Calculations were performed using the Newton code developed at Orsay University. In order to calculate the viscosity coefficients, four different and independent initial configurations were used; hence, the values presented here correspond to the average of the obtained results for the four different configurations together with the corresponding standard deviations.

Force Center Optimization. Lennard-Jones parameters were optimized following the procedure proposed by Bourasseau et al.[14] The general idea is to minimize an error criterium (F) defined as in eq 10, with respect to the L-J parameters. In this case, F is an implicit function of σ, ϵ, and δ for secondary amines, while for tertiary amines it is only a function of σ and ϵ.

$$F = \frac{1}{n}\sum_{i=1}^{n}\frac{(X_i^{sim} - X_i^{exp})^2}{s_i^2} \tag{10}$$

where n is the total number of reference data, X_i^{sim} is the value obtained from the simulations, X_i^{exp} is the experimental data, and s_i is the estimated statistical uncertainty on the computed variable X_i^{sim} ($s_i = 0.01$ for $\ln(P_v)$, $s_i = 0.5$ kJ/mol for vaporization enthalpies, and $s_i = 10$ kg/m^3 for ρ_L).

Three Lennard-Jones parameters—ϵ, σ, and δ—were optimized for the secondary amino group based on three reference molecules as a training set: dimethyl, diethyl, and di-*n*-propylamine. Vaporization enthalpies, vapor pressures, and liquid densities were selected as the thermodynamic properties to be reproduced. For each molecule, two simulations were performed at two different temperatures, namely, 260 and 350 K for dimethylamine, 300 and 400 K for diethylamine, and 375 and 470 K for di-*n*-propylamine. The same procedure was followed for tertiary amines using trimethylamine, triethylamine, and tri-*n*-propylamine as a training set. Since no hydrogen belongs to the amino group, only two L-J parameters ϵ and σ need to be optimized. For this case, the selected properties were calculated at the following temperatures: 260 and 360 K for trimethylamine, 330 and 450 K for triethylamine, and 360 and 460 K for tri-*n*-propylamine.

3. RESULTS

Unlike primary amines, for which a lot of thermodynamic phase equilibrium data is available, for secondary and tertiary amines, both experimental information and predicted values are scarce within the open literature. Nevertheless, we have managed to include a substantial set of molecules in this work in order to check the force field transferability. It is also important to mention that the force field presented in this work is not restricted to the set of molecules we have studied here, mainly because the presented set of torsions covers a large range of possible molecules.

Temperature−density phase equilibrium diagrams as well as other saturated properties such as vaporization enthalpies and vapor pressures were calculated at different temperatures for a large set of molecules in addition to the ones used for adjusting the L-J parameters. Among the set of molecules, we have included dimethylamine, diethylamine, di-*n*-propylamine, di-iso-propylamine, di-iso-butylamine for monofunctional secondary amines and trimethylamine, triethylamine, tri-*n*-propylamine, and methyldiethylamine for monofunctional tertiary amines. We have also included a multifunctional molecule involving different amino groups at the same time; this is the case of diethylenetriamine (DETA) (see Figure 3). This molecule is used in different industrial applications such as ion exchange resins, chelating agents, fuel additives, and corrosion inhibitors, among others. Figure 3 gives a schematic representation for DETA in terms of our AUA model. As can be inferred from the figure, this is a molecule with a high degree

dx.doi.org/10.1021/jp302972p | J. Phys. Chem. B 2012, 116, 6193−6202

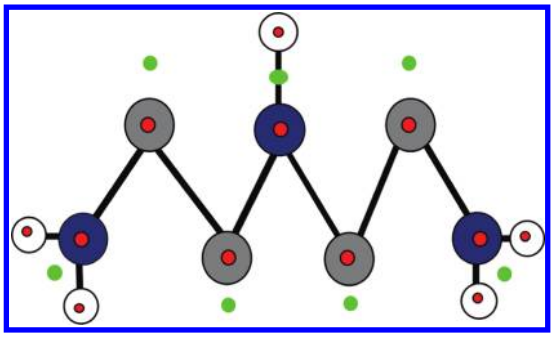

Figure 3. Schematic representation of diethylenetriamine (DETA). Green and red filled circles represent the L-J force centers and partial charges, respectively. Force centers were located according to the AUA4 rules; partial charges are located on the atoms.

of complexity, since, first, it involves two primary and one secondary amino groups and, second, because all of the involved atoms are charged. Using the AUA4 approach, 7 force centers and 12 partial charges are required for each DETA molecule. Intramolecular electrostatic interactions were calculated by means of the local dipole approach proposed by Ferrando.[20] The fully transferable model from our previous work for the primary amino groups was used without performing any additional refitting.

In the following section, we present the optimized parameters, their capability to predict the above-mentioned thermodynamic properties, and the predictions for normal boiling points and critical coordinates. Finally, we present the viscosity coefficients obtained as a function of temperature for dimethylamine, diethylamine, di-*n*-propylamine, trimethylamine, triethylamine, and tri-*n*-propylamine.

3.1. Optimization and Transferability. For secondary amines, three L-J parameters were optimized for the nitrogen of the amino group. These parameters correspond to the energy ϵ, the van der Waals radius σ, and the AUA displacement δ. After an iterative process, a set of optimized parameters for this force center was found, with ϵ = 120.66 K, σ = 3.172 Å, and δ = 0.497 Å which gives an error criterion (F in eq 10) of 1.5, validating our numerical optimization. With regards to tertiary amines, since there are no hydrogens present in the amino group, only two parameters needed to be optimized, obtaining ϵ = 47.00 K and σ = 2.600 Å with an error criterion of 1.6.

In order to check the transferability of our force field with the optimized parameters, different molecules were tested at different temperatures. A comparative table with all the molecules studied, numerical values, and corresponding errors and temperatures can be found in the Supporting Information.

3.2. Thermodynamic Properties. For all the molecules studied, temperature−density liquid−vapor equilibrium diagrams, vaporization enthalpies ,and vapor pressures were estimated. Figure 4 gives the liquid−vapor phase diagrams, Figure 5 the vaporization enthalpies, and the vapor pressures are given in Figure 6. In all cases, a comparison with the available experimental information was made.[2,37]

From the figures, it is possible to verify that the transferability for both secondary and tertiary amines is very good for all the properties studied. In short, we have obtained a global absolute average deviation (AAD = $X^{exp} - X^{sim}/X^{exp}$) over all the molecules of 1.2% for the liquid densities (ρ_L), 10.6% for the vapor pressures (P_v), and 3.5% for the vaporization enthalpies (ΔH). It is important to mention that the vaporization enthalpies we compare our simulation results to for di-iso-propylamine, di-iso-butylamine, diethylenetriamine, methyldiethylamine, and tri-*n*-propylamine are based on predicted values with associated uncertainties of 5, 10, 10, 10, and 5%, respectively. These values are in general higher than the obtained deviations with our proposed force field. For the case of DETA, the agreement between our simulation values and the experimental ones was very good for all the properties. These results confirm the capability of the force field to correctly predict the properties of molecules that do not belong to the training set. They also reaffirm the high accuracy obtained with the AUA4 force field for primary amines. The numerical values for each molecule and each temperature can be consulted in the Supporting Information.

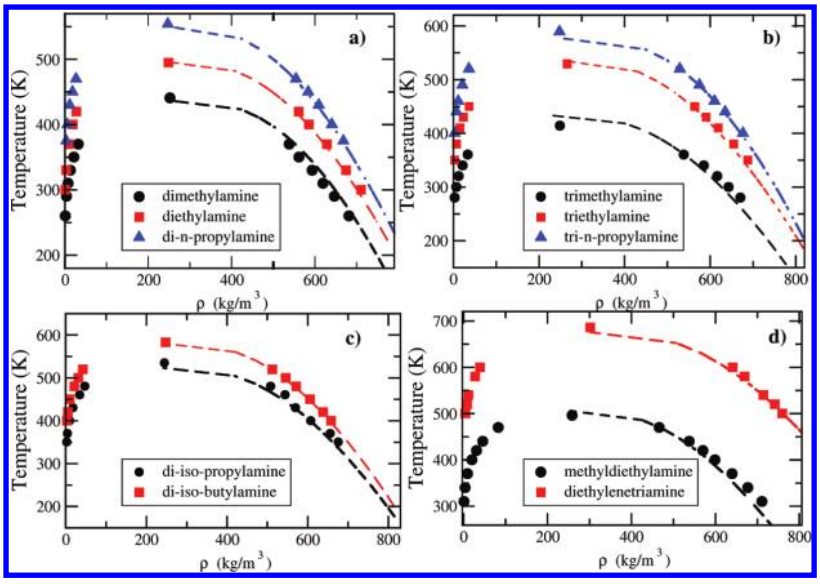

Figure 4. Comparison between experimental and AUA4 force field phase equilibrium diagrams. In all cases, the dashed lines correspond to the DIPPR experimental correlations[2] except for methyldiethylamine which is based on a proposed DIPPR prediction by means of the Racket equation with an associated uncertainty of 10%.

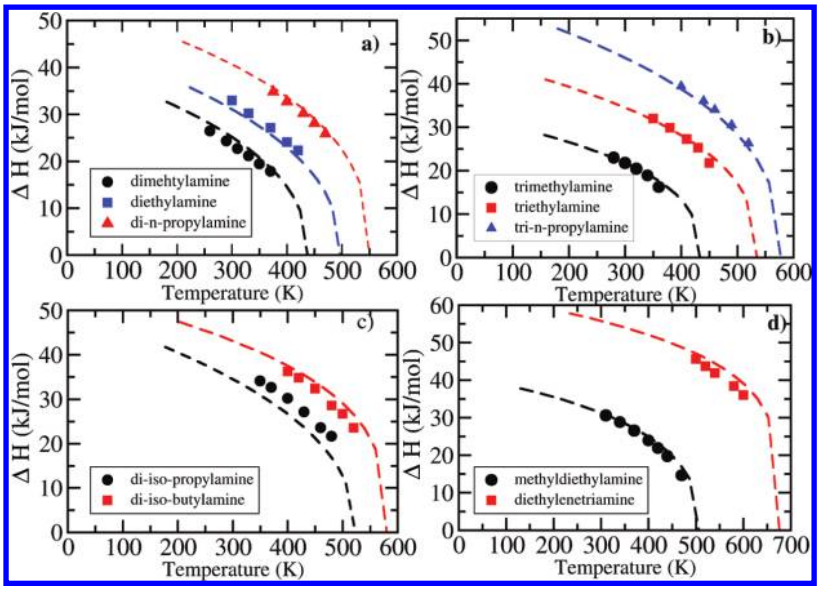

Figure 5. Comparison between experimental and AUA4 force field vaporization enthalpies. In all cases, the dashed lines correspond to the DIPPR experimental correlations.[2] For di-iso-propylamine, di-iso-butylamine, diethylenetriamine, methyldiethylamine, and tri-*n*-propylamine, the lines are predicted values.[2]

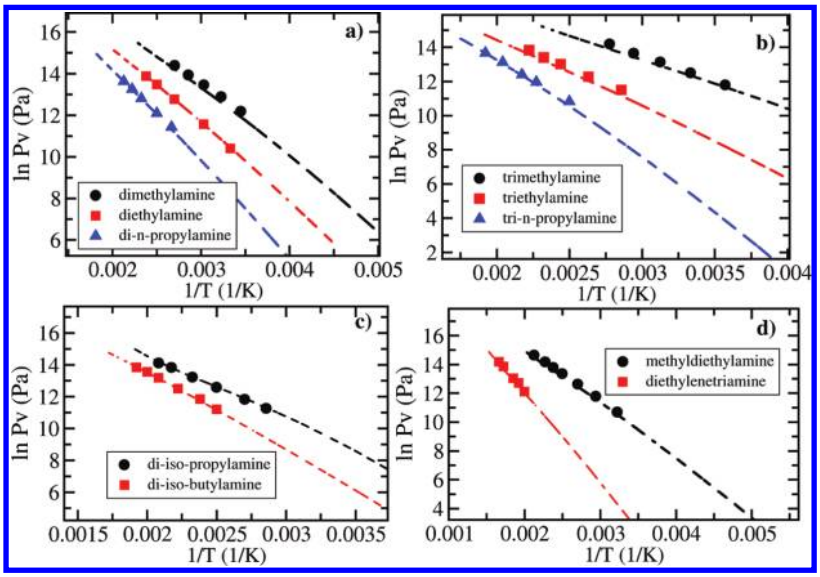

Figure 6. Comparison between experimental and AUA4 force field vapor pressures. In all cases, the dashed lines correspond to the DIPPR experimental correlations.[2]

3.3. Critical Points and Normal Boiling Points. We have calculated the critical coordinates (critical temperature and critical density) using the scaling law previously defined in eqs 8 and 9. Normal boiling points (Tb) have been calculated using the Clausius−Clapeyron equation, eq 7. Table 6 summarizes the obtained values. Nearly all the comparisons were done with experimental information,[2] except for the values with superscript *b*'s, which correspond to predictions[2] where the associated uncertainties vary between 3 and 10%. The critical pressures were also calculated from our simulation results and can be found in the Supporting Information.

In order to make a more exhaustive comparison, we have also included in Table 6 some of the results obtained for the primary amines. As can be seen, the proposed force field is also able to reproduce several important qualitative experimental features: (i) methyl, dimethyl, and trimethylamine have very close normal boiling points, dimethylamine having the highest one; (ii) with regard to the ethyl and propyl series, it is possible to see how the force field correctly reproduces the increase of the normal boiling point as the number of alkyl groups increases (from primary to tertiary amines); (iii) both the normal boiling point and the critical temperature of the branched amines are smaller than the values of their corresponding linear isomers; (iv) finally, with respect to diethylenetriamine, the obtained accuracy of the predicted values is also very good, which ratifies once again the transferability of our force field for primary amines and emphasizes the capability of our force field to also correctly predict the properties of multifunctional amines.

3.4. Viscosity Coefficients. Viscosity coefficients were calculated using molecular dynamic simulations at five different temperatures and atmospheric pressure. Figures 7 and 8 show a

dx.doi.org/10.1021/jp302972p | J. Phys. Chem. B 2012, 116, 6193−6202

Table 6. Critical Coordinates and Normal Boiling Points, Comparison between Experimental or Predicted Values and Calculations Using the AUA4 Force Field for Amines

	Tc (K)		ρ_c (kg/m^3)		T_b (K)	
molecule	exp	sim	exp	sim	exp	sim
MA[a]	431	433_3	232	234_3	267	269_2
DMA	437_4	441_2	251_7	252_4	280_6	273_2
TMA	433_4	414_3	233_6	249_5	276_3	266_3
EA[a]	456	458_2	244	251_5	290	294_3
DA	496_5	495_3	243_5	248_2	329_3	330_2
TA	536_5	529_3	259_{11}	266_6	362_8	358_3
PA[a]	497	495_2	na	260_5	321	319_2
DPA	555_{10}	554_3	252_9[b]	247_5	382_9	379_3
TPA	597_{14}	589_3	247_7[b]	248_3	430_4	428_2
iso-PA[a]	472	469_3	267	265_4	304	304_1
DIPA	523_5	535_4	249_{11}[b]	245_6	357_{12}	356_2
DIBA	584_{10}[b]	583_4	250_{11}[b]	248_4	412_{12}	409_3
DETA	676_{20}[b]	686_4	302_{15}[b]	302_3	480_5	475_2
MDA	509_{18}[b]	496_3	251_7[b]	259_2	339_1[b]	332_2

[a]Values taken from the AUA4 force field for primary amines.[24] [b]DIPPR predicted values. Experimental values taken from DIPPR and NIST databases,[2,37] na = not available. MA = methylamine, DMA = dimethylamine, TMA = trimethylamine, EA = ethylamine, DA = diethylamine, TA = triethylamine, PA = *n*-propylamine, DPA = di-*n*-propylamine, TPA = tri-*n*-propylamine, iso-PA = iso-propylamine, DIPA = di-iso-propylamine, DIBA = di-iso-butylamine, DETA = diethylenetriamine, MDA = methyldiethylamine. The subscripts give the statistical uncertainties of the last digit(s).

comparison between the experimental (gray filled circles) and the simulated (open circles) viscosity coefficients for secondary and tertiary amines, respectively. Note that the viscosities are given in centipoise. Six molecules were studied in total, namely, dimethyl, diethyl, and di-*n*-propylamine for secondary amines and trimethyl, triethyl, and tri-*n*-propylamine for tertiary amines. The experimental information for diethyl, di-*n*-propyl, triethyl, and tri-*n*-propylamine were taken from the works by Shah et al.[38] and Oswal et al.,[39] while for dimethyl and trimethylamine the values were taken using the correlation from the DIPPR database[2] which is based on the experimental work reported by Swift et al.[40] For all the simulated molecules, both the Green−Kubo and the Einstein formalisms were employed to calculate the viscosity coefficients. As expected, the results obtained from both formalisms were numerically equivalent within the statistical uncertainty. The obtained numerical values are given in the Supporting Information.

As can be inferred from Figures 7 and 8, the simulation values are in very good agreement with the experimental information. For secondary amines and tertiary amines, we have obtained a global average deviation of 3.2 and 6.6%, respectively . This fact highlights the capability of our model to predict not only thermodynamic properties but also transport properties.

4. CONCLUSIONS AND PROSPECTS

In this work, we have developed a new force field for secondary and tertiary amines following the anisotropic united atom approach that includes only one force center per functional group. The force field uses three and two L-J parameters to model the amino group of secondary amines and tertiary amines, respectively. Different sets of partial charges are proposed for the amino group in secondary and tertiary amines due to the different dipole moments found in the liquid phase. We have also developed a set of torsions that allowed us to study 10 different amine molecules. We would like to emphasize that these torsions allow our force field to be applied to a large number of additional molecules beyond those included in this work.

The force field shows, in general, an excellent capability in predicting thermodynamic properties such as densities, vaporization enthalpies, and vapor pressures compared with available experimental data. It is also able to reproduce with high accuracy the critical coordinates and normal boiling points, including the correct physical qualitative tendencies of the homologous series for primary, secondary, and tertiary amines. It is also able to reproduce correctly the behavior of

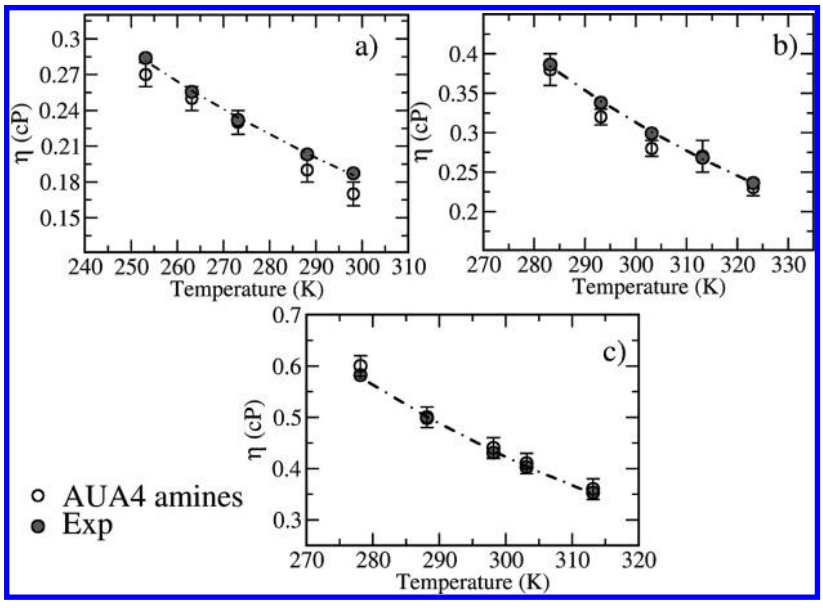

Figure 7. Shear viscosity as a function of temperature: (a) dimethylamine; (b) diethylamine; (c) di-*n*-propylamine. The dashed line is shown as a guide for the reader.

dx.doi.org/10.1021/jp302972p | J. Phys. Chem. B 2012, 116, 6193−6202

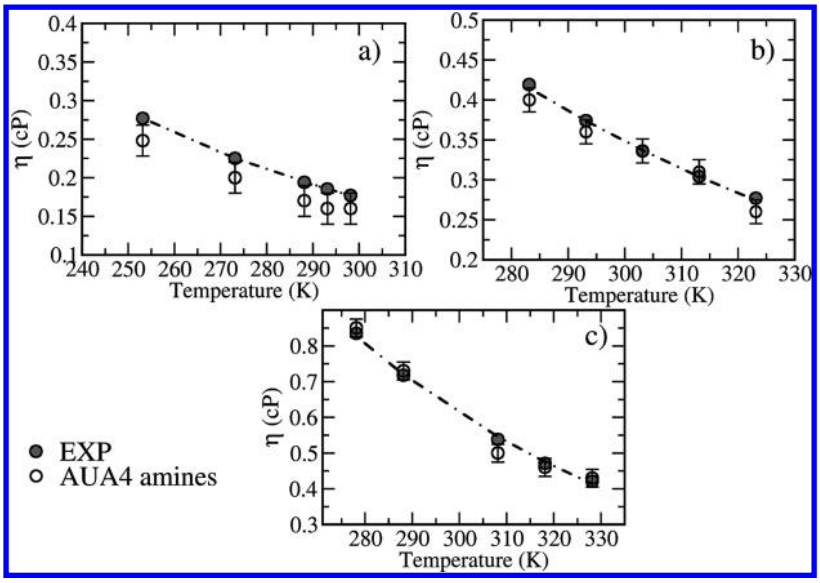

Figure 8. Shear viscosity as a function of temperature: (a) trimethylamine; (b) triethylamine; (c) tri-*n*-propylamine. The dashed line is shown as a guide for the reader.

multifunctional amines such as diethylenetriamine, demonstrating the consistency of our force field between the primary and secondary amino groups.

Finally, the viscosity coefficients calculated from the molecular dynamics simulations have also shown a very good agreement with the experimental values for the studied molecules as a function of temperature. This demonstrates that the AUA4 model is able to predict not only thermodynamic properties but also transport properties at the same time.

Further work is currently in progress to extend the AUA4 model to alkanolamines.

■ ASSOCIATED CONTENT

Supporting Information

Simulation results and experimental values of saturated liquid densities, vaporization enthalpies, vapor pressures, and viscosities are given for all the studied molecules at different temperatures. This material is available free of charge via the Internet at http://pubs.acs.org.

■ AUTHOR INFORMATION

Corresponding Author

*E-mail: veronique.lachet@ifpen.fr.

Notes

The authors declare no competing financial interest.

■ ACKNOWLEDGMENTS

G.A.O. acknowledges IFP Energies nouvelles for his Ph.D. grant. A.D.M. acknowledges financial help from the Spanish Ministry of Science and Innovation MICINN via project CTQ2008-06469/PPQ. The authors would like to thank Dr. Bernard Rousseau for the use of the Newton MD code.

■ REFERENCES

(1) Rizzo, R. C.; Jorgensen, W. L. *J. Am. Chem. Soc.* **1999**, *121*, 4827−4836.
(2) Rowley, R.; Wilding, W. L.; Oscarson, J. L.; Danner, R. P. *Design Institute for Physical Properties*; AIChE: New York, 1987.
(3) Wick, C. D.; Stubbs, J. M.; Neeraj, R.; Siepmann, J. I. *J. Phys. Chem. B* **2005**, *109*, 18974−18982.
(4) Schnabel, T.; Vrabec, J.; Hasse, H. *Fluid Phase Equilib.* **2008**, *263*, 144−159.
(5) Ungerer, P.; Tavitian, B.; Boutin, A. *Applications of molecular simulation in the Oil and Gas Industry*; Technip: Paris, 2005; p 267.
(6) Baskaya, F. S.; Gray, N. H.; Gerek, Z. N.; Elliot, J. R. *Fluid Phase Equilib.* **2005**, *236*, 42−52.
(7) Toxvaerd, S. *J. Chem. Phys.* **1990**, *93*, 4290−4295.
(8) Ungerer, P.; Beauvais, C.; Delhommelle, J.; Boutin, A.; Rousseau, B.; Fuchs, A. H. *J. Chem. Phys.* **2000**, *112*, 5499−5510.
(9) Mackie, A. D.; Tavitian, B.; Boutin, A.; Fuchs, A. H. *Mol. Simul.* **1997**, *19*, 1−15.
(10) Contreras-Camacho, R. O.; Ungerer, P.; Boutin, A.; Mackie, A. D. *J. Phys. Chem. B* **2004**, *108*, 14109−14114.
(11) Ahunbay, M. G.; Pérez-Pellitero, J.; Contreras-Camacho, R. O.; Teuler, J. M.; Ungerer, P.; Mackie, A. D.; Lachet, V. *J. Phys. Chem. B* **2005**, *109* (7), 2970−2976.
(12) Delhommelle, J.; Tschirwitz, C.; Ungerer, P.; Granucci, G.; Millie, P.; Pattou, D.; Fuchs, A. H. *J. Chem. Phys.* **2000**, *104*, 47454−753.
(13) Nieto-Draghi, C.; Ungerer, P.; Rousseau, B. *J. Chem. Phys.* **2006**, *125*, 1−15.
(14) Bourasseau, E.; Haboudou, M.; Boutin, A.; Fuchs, A. H.; Ungerer, P. *J. Chem. Phys.* **2003**, *118*, 3020−3034.
(15) Bourasseau, E.; Ungerer, P.; Boutin, A. *J. Phys. Chem. B* **2002**, *106*, 5483−5491.
(16) Bonnaud, P.; Nieto-Draghi, C.; Ungerer, P. *J. Phys. Chem. B* **2007**, *111*, 3730−3741.
(17) Pérez-Pellitero, J.; Ungerer, P.; Mackie, A. D. *J. Phys. Chem. B* **2007**, *111*, 4460−4466.
(18) Pérez-Pellitero, J.; Bourasseau, E.; Demachy, I.; Ridard, I.; Ungerer, P.; Mackie, A. D. *J. Phys. Chem. B* **2008**, *112*, 9853−9863.
(19) Boutard, Y.; Ungerer, P.; Teuler, J. M.; Ahunbay, M.; Sabater, S.; Pérez-Pellitero, J.; Mackie, A. D.; Bourasseau, E. *Fluid Phase Equilib.* **2005**, *236*, 25−41.
(20) Ferrando, N.; Lachet, V.; Teuler, J. M.; Boutin, A. *J. Phys. Chem. B* **2009**, *113*, 5985−5995.
(21) Ferrando, N.; Lachet, V.; Boutin, A. *J. Phys. Chem. B* **2009**, *114*, 8680−8688.
(22) Ferrando, N.; Lachet, V.; Boutin, A. *J. Phys. Chem. B* **2011**, *115*, 10654−10664.
(23) Ferrando, N.; Lachet, V.; Boutin, A. *J. Phys. Chem. B* **2012**, *116*, 3239−3248.

(24) Orozco, G. A.; Nieto-Draghi, C.; Mackie, A. D.; Lachet, V. *J. Phys. Chem. B* **2011**, *115*, 14617−14625.
(25) *Jaguar*, version 7.7; Schrodinger, LLC: New York, 2010.
(26) Mclellan, A. *Table of experimental dipole moments*; W. H. Freeman and Co.: New York, 1963; Vols. *I*−*III*.
(27) Tannor, D. J.; Marten, B.; Murphy, B.; Friesner, R. *J. Am. Chem. Soc.* **1994**, *116*, 11875−11882.
(28) Wyman, J., Jr. *J. Am. Chem. Soc.* **1936**, *58* (8), 1482−1486.
(29) Sild, S.; Karelson, M. *Chem. Inf. Comput. Sci.* **2002**, *42*, 360−367.
(30) Chen, K. H.; Lii, J. H.; Fan, Y.; Allinger, N. L. *J. Comput. Chem.* **2007**, *28*, 2391−2412.
(31) McKean, D. C. *J. Chem. Phys.* **1983**, *79* (4), 2095−2096.
(32) Fujiwara, H.; Egawa, T.; Konaka, S. *J. Mol. Struct.* **1995**, *344*, 217−226.
(33) Takeuchi, H.; Kojima, T.; Egawa, T.; Konaka, S. *J. Phys. Chem.* **1992**, *96*, 4389−4396.
(34) Batista de Carvalho, L. A. E.; Texeira-Dias, J. J. C.; Fausto, R. *Struct. Chem.* **1990**, *1*, 533−542.
(35) Frenkel, D.; Smit, B. *Understanding molecular simulations*; Academic Press: New York, 2002; p 201.
(36) Andersen, H. *J. Chem. Phys.* **1983**, *52*, 2−34.
(37) http://cccbdb.nist.gov.
(38) Shah, J.; Dewitt, J.; Stoops, C. *J. Chem. Eng. Data* **1969**, *14*, 333−335.
(39) Oswal, S. L.; Sindhe, R. G.; Patel, A. T.; Dave, J. P.; Patel, S. G.; Patel, B. M. *Int. J. Thermophys.* **1992**, *13*, 617−628.
(40) Swift, E; Dexter, L. W. *J. Am. Chem. Soc.* **1944**, *66*, 498−499.